CONFERENCE PRE-PRINT

PUMPING REQUIREMENTS FOR CORE PLASMA PERFORMANCE IN STEP USING JINTRAC

¹E. THOLERUS, ¹R. FUTTERSACK, ¹S.S. HENDERSON, ¹D. MOULTON, ¹F.J. CASSON, ¹A. HUDOBA, ²F. KOECHL, ¹S.P. MARSDEN, ¹O. MYATRA, ¹R.T. OSAWA, ¹J. SIMPSON, ³A. TARAZONA, ¹L. XIANG

¹UKAEA (United Kingdom Atomic Energy Authority), Culham Campus, Abingdon, OX143DB, UK

Email: emmi.tholerus@ukaea.uk

Abstract

STEP is a prototype power plant that is intended to demonstrate $\sim 100\,\text{MW}$ of net electricity production during steady-state operation. A crucial aspect of the design is the efficiency of the helium pumping, since it defines the degree of helium dilution in steady-state, and the resulting pumped flux sets an upper bound of the fusion reaction rate. In this work, the JIN-TRAC core/SOL/pump/divertor integrated model has been used to quantify the required helium pumping speed for sufficient fusion power performance. Complementary studies have been done with core-only JETTO simulations to account for uncertainties in the confinement and pedestal assumptions. The combined results have been used to estimate a minimum required helium pumping speed as a function of confinement factor and normalised pressure gradient in the edge plasma. Based on the most recent set of confinement and pedestal assumptions for STEP, the presented modelling indicates a minimum required helium pumping speed of around 50 m³/s. While this value is significantly larger than in any present day experiment, it is in line with the assumption for ITER.

1. INTRODUCTION

The interplay between pump and core plasma in tokamaks is a highly integrated problem, requiring consistent plasma solutions from the magnetic axis all the way to the pump via the scrape-off layer (SOL). This is a crucial problem for any DEMO-class reactor, such as the Spherical Tokamak for Energy Production (STEP), which requires efficient pumping of helium ash to avoid degradation of fusion power performance due to impurity dilution. STEP is intended to demonstrate net electric output power of the order 100 MW during steady-state flat-top operation, which means that the total fusion power will need to significantly exceed the power required for heating, fuelling and coil systems to account for various loss mechanisms [1]. JINTRAC [2], which is a unique tool for integrated core, edge, SOL, pump and divertor modelling, has been used in this work to model α -particle generation, thermalisation and transport to the pump surfaces. The benefits of running a core/SOL/pump integrated model as opposed to a core-only plasma model are that self-consistent boundary conditions can be applied at the last closed flux surface, and quantitative pump parameters, such as the pumping speed, can be directly correlated with core plasma performance. If the study reveals that the required pumping speed cannot be achieved due to technical limitations, the design of the exhaust systems, and possibly the whole tokamak, might need to be reassessed. Another option would be to develop scenarios with higher helium compression (ratio of helium density in the divertor and the main chamber) to increase the helium throughput.

A comprehensive overview of the STEP exhaust scenario, including divertor and pump designs, is presented in [3]. Deuterium, tritium and non-helium impurities will be pumped via a cryopump system, whereas helium is carried via separate turbomolecular pumps to the rest of the fuel cycle, meaning that the pump system designs can be optimised separately for helium ash and for other species. The helium pumping efficiency is quantified using the pumping speed parameter $S_{\rm He}$ (units of m³/s). It is related to the pump albedo $A_{\rm He}$, i.e., the fraction of reflected to incident helium atom at the pump surface, according to

$$S_{\text{He}} = \Sigma_{\text{pump}} (1 - A_{\text{He}}) \sqrt{\frac{T_0}{2\pi m_{\text{He}}}},\tag{1}$$

²ITER Organization, Route de Vinon-sur-Verdon, CS 90046, 13067 St. Paul Lez Durance Cedex, France

³UK Industrial Fusion Solutions Ltd, Culham Campus, Abingdon, OX14 3DB, UK

where Σ_{pump} is the total area of the pump, T_0 is the neutral temperature at the pump surface, and m_{He} is the mass of the helium atom. Using the above definition, the pumped flux (number of pumped helium atoms per second) is simply

$$\Gamma_{\rm He} = S_{\rm He} n_{\rm He^0,pump},\tag{2}$$

where $n_{\rm He^0,pump}$ is the helium neutral density by the pump. The ASDEX Upgrade turbomolecular pump systems for helium removal have achieved pumping speeds of around 7 m³/s [4], whereas ITER works with the assumption of cryopump systems that support $S_{\rm He} > 52\,{\rm m}^3$ /s [5].

2. MODELLING ASSUMPTIONS

2.1. Whole plasma integrated modelling with JINTRAC

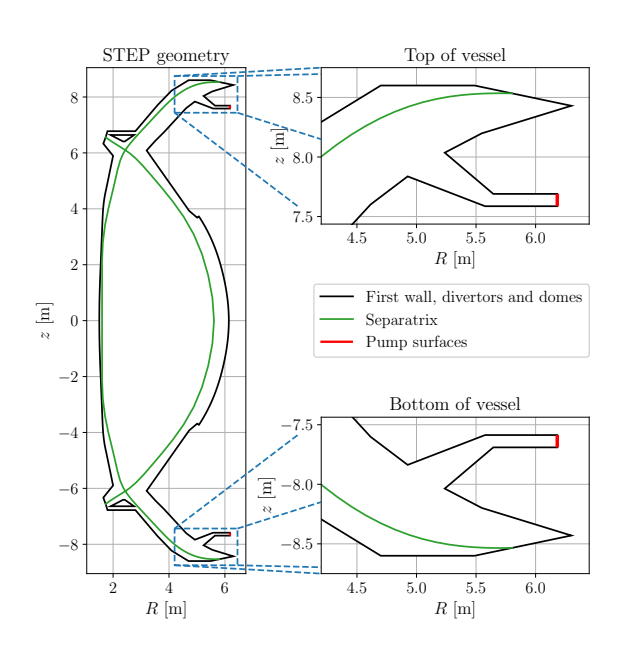


FIG. 1. Vacuum vessel geometry and pump locations.

JINTRAC is the whole plasma integrated framework that consists of JETTO [6] for core plasma modelling, and EDGE2D/EIRENE [7, 8] for modelling of plasma and neutrals in the SOL, for gas puffing and pumping, and for sputtering/recycling from the divertors and first wall. JETTO and EDGE2D/EIRENE are coupled at runtime via boundary conditions applied at the last closed flux surface. The adaptive time stepping is controlled by EDGE2D, which generally needs to resolve the shortest time scale variations of plasma densities and temperatures. In addition, a partial coupling scheme is used between JETTO and EDGE2D/EIRENE for higher computational efficiency, in which EDGE2D/EIRENE is only advanced for a fraction of the total plasma time within regular intervals of the ms time scale. The presented simulations operate in 4 ms intervals, where EDGE2D/EIRENE and JETTO are fully coupled for 1 ms. During the remaining 3 ms of the interval, JETTO advances on its own, while any SOL fluxes are extrapolated in time.

Fig. 1 illustrates the full geometry of the first wall, divertors and pump surfaces that have been assumed in the presented JINTRAC simulations, which matches

the latest iteration of the designs in [3]. It includes a highly elongated plasma ($\kappa \approx 3$), with up-down symmetric geometry, double-null divertors and extended outer legs. Active pumping is limited to the outer divertor regions, and dome structures are included to direct the neutral flow between the inner and outer divertor regions. The total pump area is $8.03\,\mathrm{m}^2$, and the neutral temperature at the pump surfaces is set to $580\,\mathrm{K}$. Four test cases have been set-up with S_{He} taking the values 12, 48, 192, and $768\,\mathrm{m}^3/\mathrm{s}$, respectively. Pumping of non-helium species (deuterium, tritium and argon, including molecular compositions) is defined by a fixed albedo of 0.993176. No sputtering of wall/divertor impurities have been considered in the presented simulations, for computational efficiency.

The core plasma assumptions are similar to those used in [9] for the EC-HD scenario. Confinement has been assumed by rescaling of Bohm/gyro-Bohm on feedback against a target $\beta_{\rm N}=\beta_{\rm N,th}+\beta_{\rm N,\alpha}$, as described in the reference. This kind of assumption allows for improved stability of the scenarios, and faster convergence, which is prioritised because of the computational requirements for running core/SOL/divertor/pump integrated JINTRAC. The viability of the resulting confinement assumption can in principle be tested by comparing the confinement time against empirical scaling laws. The D/T pellet fuelling has been modelled by a continuous Gaussian source in $\rho_{\rm tor}$, with the source rate on feedback against a target line averaged electron density of $1.6\times10^{20}~{\rm m}^{-3}$. A reduced charge state model [10] has been used for efficient solving of the momentum equations for multiple impurity species in EDGE2D, whereas the core impurity transport is primarily neoclassical, predicted with NCLASS [11]. Perpendicular particle transport in the SOL is computed with interpolated diffusivity profiles as described in [12], rather than predicted from drift equations.

The main difference of the presented JINTRAC simulations compared to the previous EC-HD scenario is that they exclude the seeding of xenon, which is done for improved numerical stability and efficiency. Xenon is the primary radiation source from the core, which is used to enable detachment access. With the exclusion of xenon, the core radiation is set to a value corresponding to 70% of the total heating power (auxiliary, α -heating, and

ohmic power), and at a constant radiation power density. Another difference is that the target β_N value for feedback against the Bohm/gyro-Bohm transport is set to 4.4 rather than 4.5. For a more complete description of the core plasma modelling assumptions, including descriptions of the individual models that are used in integration, please see [9].

2.2. Parameter scan with core-only model JETTO

In addition to the helium dilution in the core plasma, the fusion power performance depends largely on the confinement assumptions. A plasma with high heat confinement can sustain a larger degree of helium dilution at a given electron density, since the reduced D/T density due to dilution can be compensated by higher ion temperatures. The pedestal height can also impact the helium compression via neoclassical screening and overall peaking of the density and temperature profiles. Both the confinement and pedestal assumptions have large uncertainties, since neither of these can be verified against present-day experiments in any STEP relevant operation regime (DEMO-class spherical tokamak). It would be computationally unfeasible to scan the whole parameter space of varying confinement and pedestal assumption in conjunction with varying helium pumping efficiency using fully integrated core and SOL/divertor/pump modelling with JINTRAC. Instead, complementary studies have been done with JETTO core-only simulations to study the impact of confinement and pedestal assumption on fusion power performance. Combining these results with the JINTRAC scan in helium pumping speed can provide a more complete understanding of the required pumping efficiencies for a range of modelling assumptions.

To perform the scan in confinement assumption, the Bohm/gyro-Bohm transport has been scaled on feedback against the total fusion power with a target value of 1.5 GW, while simultaneously varying the helium concentration at the last closed flux surface (LCFS). 1.5 GW is the assumed lower limit for sufficient fusion power performance for STEP [9]. Since JETTO is core-only, ion densities at the LCFS are set as boundary conditions for the simulations. Variation of the helium concentration at the LCFS effectively varies the helium concentration in the whole core at stationary conditions. Since the fusion power is fixed, the varying helium dilution in the core results in varying degrees of heat confinement. The scan in pedestal assumption is done by using a continuous ELM model in the edge transport barrier (ETB), in which the edge ballooning parameter α is limited by a set upper bound value α_{crit} by continuously amplifying the diffusivities in the ETB region on feedback against α .

The helium concentration is varied by increasing the helium density while decreasing the D/T densities at the LCFS in such a way that the electron density is approximately fixed at $3\times 10^{19}~\text{m}^{-3}$. Since the fraction of helium that is not fully ionised is free to vary between scenarios, the resulting electron density at the LCFS also varies slightly. Likewise, the set $\alpha_{\rm crit}$ in the continuous ELM model does not match the maximum α value in the ETB region ($\alpha_{\rm max}$) due to the gradual amplification of the diffusivities as α exceeds $\alpha_{\rm crit}$. On average, $\alpha_{\rm max}$ is about 11.5 % higher than the input $\alpha_{\rm crit}$. Shown along the axes of the scan plots in Section 3.2 are the average values of the helium concentration and $\alpha_{\rm max}$ in the ETB region along each scan dimension, respectively.

3. RESULTS

3.1. Scan in helium pumping speed with JINTRAC

Selected time traces for the four pumping speed cases are presented in Fig. 2. There is a clear separation in resulting core helium concentration for the different pumping speeds (Fig. 2.a), which demonstrates the correlation between pumping assumptions and the core plasma scenario. The helium source-sink balance in Fig. 2.c is computed as the difference between the fusion reaction rate and the pumped flux, which should reach a balance in steady-state operation, presuming that wall losses of α -particles are negligible compared to the pumped flux. While the highest pumping speed case still shows a net sink of the helium, the other cases are fairly well equilibrated. A slight separation in the resulting fusion power can be observed (Fig. 2.d), in particular following $t \approx 204$ s, where the lower pumping speed cases have a faster decline of the fusion power as a result of the increased helium dilution. The net decrease of P_{fus} for the highest pumping speed cases, despite the decreasing core averaged helium dilution, can be understood from an increased peaking of the helium concentration as the scenarios reach stationary conditions, with a higher relative dilution on-axis where the reaction rates densities are the highest. The core averaged ion temperatures (Fig. 2.e) are similar in all four cases because of the feedback on diffusivity with respect to β_N in conjunction with the pellet fuelling feedback against average electron density. However, it is difficult to observe any significant differences in the confinement factor (Fig. 2.f), since the amplitude of the oscillations in H_{98}^* are larger than any differences in the time average values between the cases. The oscillation frequencies of the confinement factor are between 0.5 and 1 Hz, which is the time scale at which the feedback in Bohm/gyro-Bohm scaling factors respond to changes in β_N . The same oscillation rates can also be observed in the fusion power and in the ion temperature.

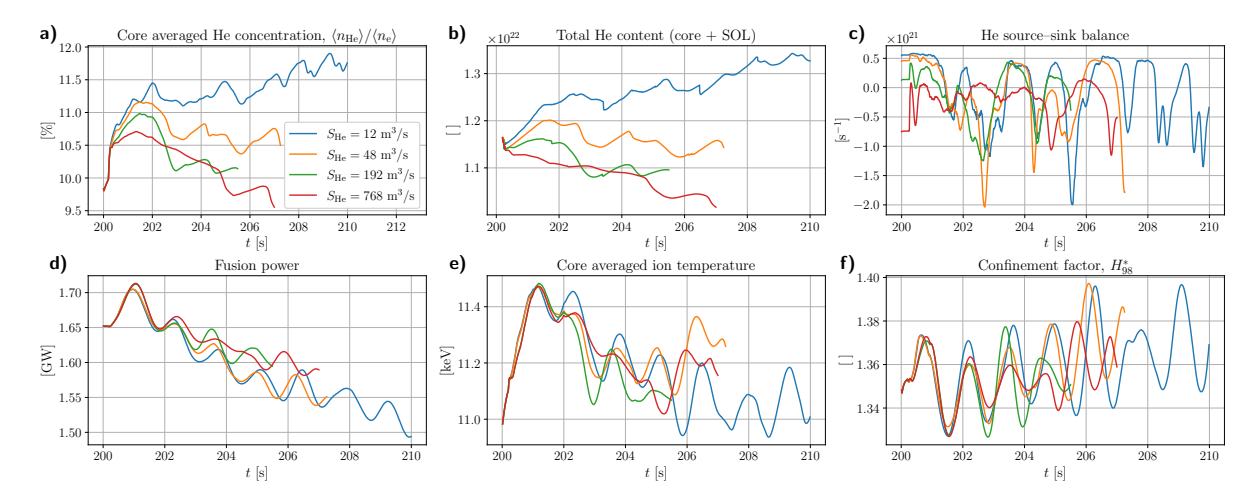


FIG. 2. Time trace data for scan in helium pumping speed with JINTRAC. The helium source—sink balance in (c) is the fusion reaction rates minus the pumped flux. The confinement factor H_{98}^* in (f) is the ITER scaling $H_{\rm IPB98(y,2)}$ with 60% of core radiation taken into account for the net power [9].

These results alone are not sufficient to draw any conclusions regarding viable pumping scenarios. However, combining them with the JETTO scan results in confinement and pedestal assumptions in Section 3.2, it is possible to do a more quantitative analysis of the pumping requirements, as demonstrated in Section 3.3.

3.2. JETTO parameter scan in helium concentration and pedestal height

The main results of the scan in $n_{\rm He,sep}$ and $\alpha_{\rm max}$ are shown in Fig. 3. The scan used 9 different values of $n_{\rm He,sep}$, and 11 values of $\alpha_{\rm max}$, totalling to $9\times 11=99$ scan points. Each scan point has been run for $100\,\rm s$, where the scenarios largely converge to stationary conditions. Fig. 3.c demonstrates a clear correlation between $n_{\rm He,sep}$ and the core averaged helium concentration in stationary conditions. Increased helium dilution leads to an increased energy confinement, as shown in Figs. 3.a and 3.b. An increased pedestal height also results in a lower core averaged helium concentration at constant $n_{\rm He,sep}$. This can be understood from the increased flattening of the kinetic profiles (see the temperature profiles in Fig. 3.d), corresponding to a more off-axis helium source. This in turn leads to a reduced confinement time for helium, resulting in a lower average dilution, as seen in Fig. 3.e.

Convergence of a simulation output is tested by comparing the final value against the time averaged value over the last 10 s of the simulation. If the final value deviates more than 1% from the time averaged value, the corresponding point is filtered out from the output, as demonstrated for the H_{98}^* data in Figs. 4.a – 4.d. The filtered H_{98}^* data has been fitted to a linear model function $C_0 + C_n n_{\rm He,sep} + C_\alpha \alpha_{\rm max}$ using the ordinary least square method. The results are shown in Fig. 4.e, which found that $C_0 = 1.35$, $C_n = 1.88 \times 10^{-20} \, \rm m^3$, and $C_\alpha = -4.09 \times 10^{-2}$. The linear assumption is expected to break towards low $n_{\rm He,sep}$, since $n_{\rm He,sep}$ cannot extend to negative values. However, the residual plot of Fig. 4 indicates that the linear model function fits reasonably well to the scan data within the studied parameter space, with a majority of the data points deviating less than 0.5% from the linear fit. The linear fit reveals a quantitative relationship between the confinement and pedestal assumptions, and the helium separatrix density.

3.3. Correlation between the minimum pumping speed and core/edge transport assumptions

To find the minimum required helium pumping speed as a function of the confinement and pedestal assumptions, we start by studying any possible correlation between pumped flux and separatrix helium density. This correlation can be combined with the approximated linear relationship between $n_{\rm He,sep}$, $\alpha_{\rm max}$ and H_{98}^* to reveal the sought dependence. The pumped flux is determined by the pumping speed and the average neutral density by the pump surface. Figs. 5.a and 5.b show the average neutral helium density at the pump and the helium density at the separatrix as a function of time for the four pumping speed cases in the JINTRAC simulations of Section 3.1, with the final 3 s of each simulation highlighted in bold. Plotting these outputs on separate axes, as is done in Fig. 5.c, appears to indicate that each scenario oscillates around stable points in this space towards the end of the simulations. For the two lower pumping speed cases, the neutral densities at the pump vary by more than an order of magnitude along these oscillations, whereas the higher pumping speed cases are more stable in $n_{\rm He^0,pump}$. The oscillations are likely correlated with the feedback in core heat confinement against $\beta_{\rm N}$. They are of similar time scales, and oscillations in the helium source rate (which is proportional to the fusion power, Fig. 2.d) can

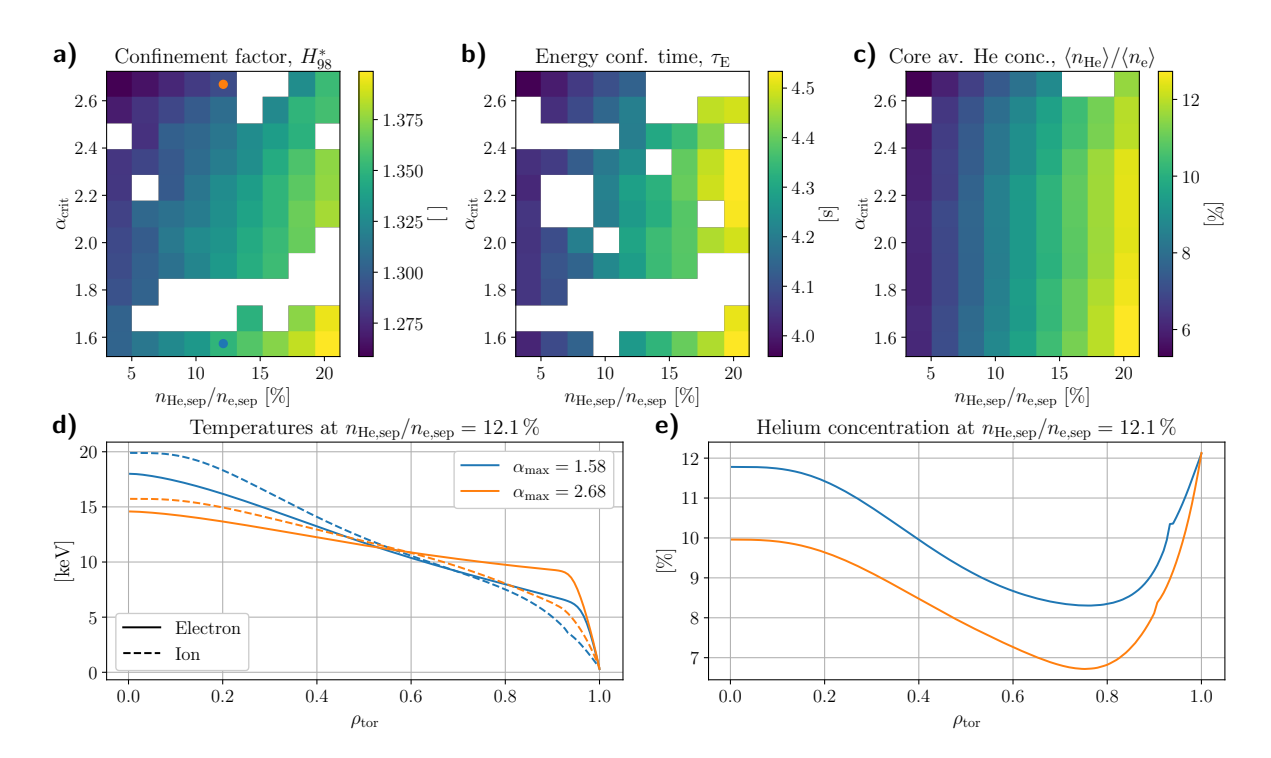


FIG. 3. Results from the scan in confinement and pedestal assumptions with JETTO. a) – c) The presented data shows the final value of H_{98}^* , $\tau_{\rm E}$, and $\langle n_{\rm He} \rangle / \langle n_{\rm e} \rangle$ in each scan point. The white points correspond to data that had not fully converged by the end of the simulation, using a filtering process demonstrated in Figs. 4.a – 4.d. d) and e) show profile data from the end of the simulations of two selected scan points (the location of the blue and orange dot in a)).

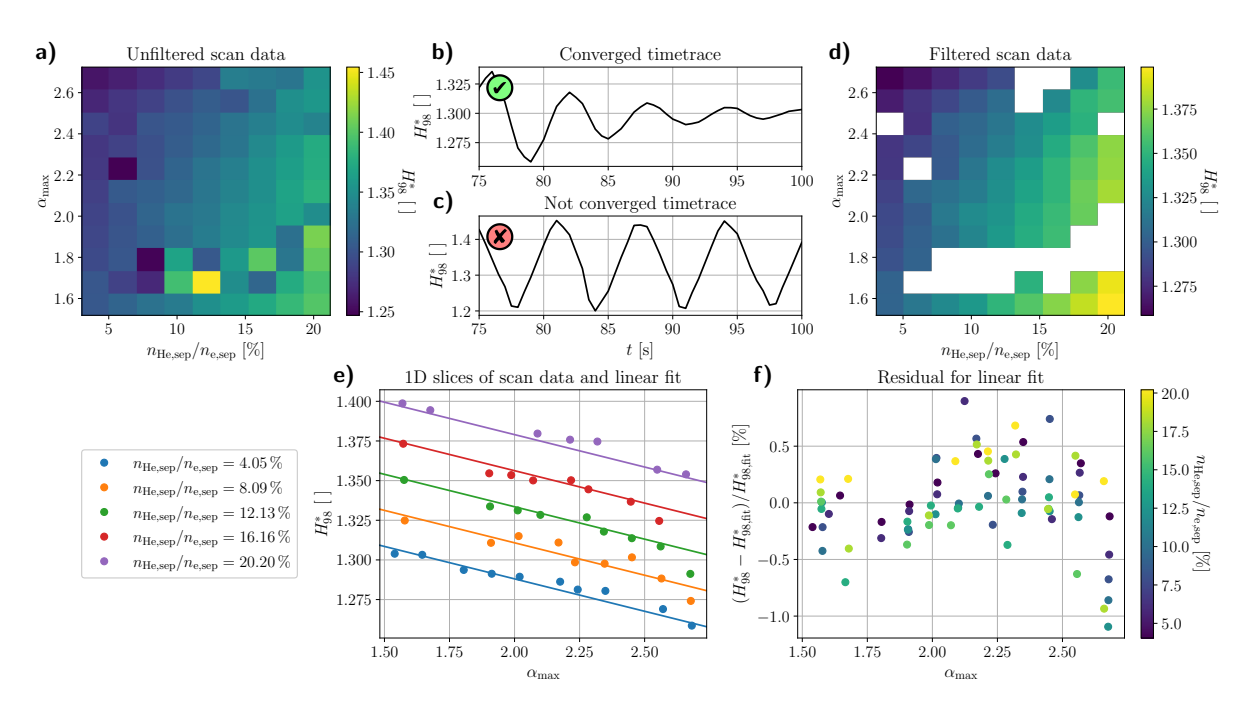


FIG. 4. a) – d) Demonstration of the filtering process for the scan data. The output of a scan point is filtered out if the final value deviates more than 1 % from the time averaged value of the last 10 s of the simulation. e) and f) Filtered H_{98}^* data fitted to a linear model function $C_0 + C_n n_{\rm He, sep} + C_\alpha \alpha_{\rm max}$.

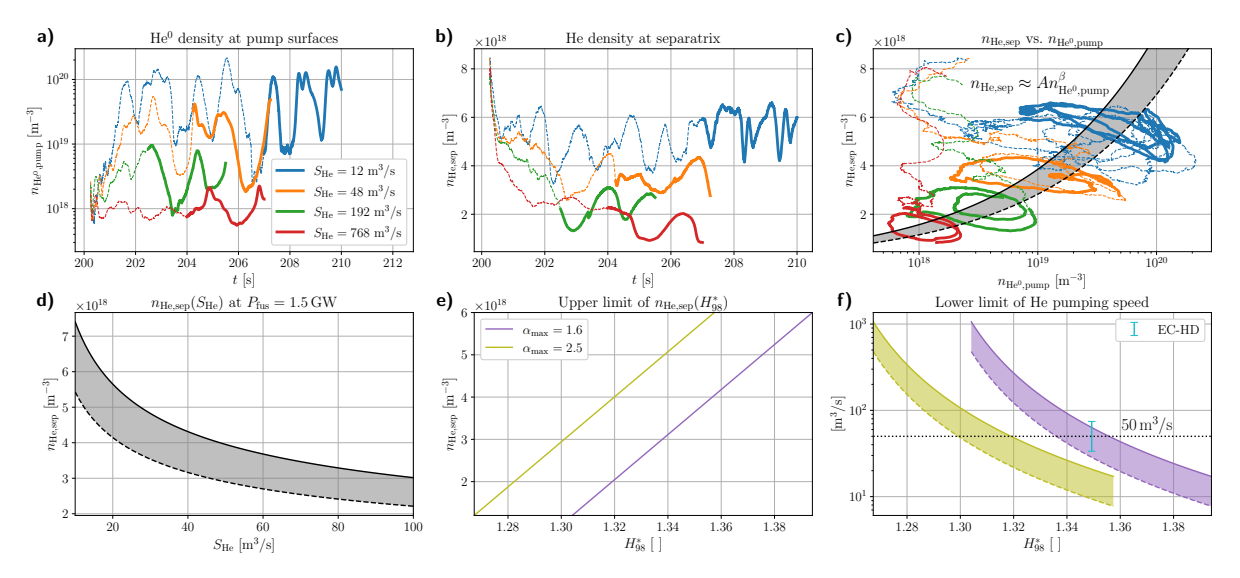


FIG. 5. a) – c) Average neutral helium density at the pump surfaces and the helium density at the separatrix for the four pumping speed cases presented in Section 3.1. The final 3 s of each simulation has been highlighted with bold, solid curves. c) also presents a suggested relationship between the stable $(n_{\rm He^0,pump}, n_{\rm He,sep})$ points with the shaded area (accounting for uncertainties). d) Helium separatrix density as a function of pumping speed, assuming a pumped flux that matches the reaction rate of $P_{\rm fus}=1.5$ GW. e) Relationship between $H_{\rm 98}^*$, $n_{\rm He,sep}$ and $\alpha_{\rm max}$ at $P_{\rm fus}=1.5$ GW, as derived in Section 3.2. f) Helium pumping speed required for a pumped flux matching the $P_{\rm fus}=1.5$ GW reaction rate as a function of $H_{\rm 98}^*$ and $\alpha_{\rm max}$, according to eq. (3). The error bar shows the corresponding $S_{\rm He}$ required for the EC-HD flat-top scenario [9], and the dotted line is the suggested practical limit of $S_{\rm He}$.

propagate to oscillations in both helium separatrix density and neutral helium density at the pump with some delay time between these.

A simple power law, $n_{\rm He,sep} = A n_{\rm He^0,pump}^{\beta}$, can be fitted to the centres of these two points. The extrapolated curve towards higher $n_{\rm He^0,pump}$ still coincides reasonably with the centres of the oscillations for the lower pumping speed cases. The shaded areas in Figs. 5.c, 5.d and 5.f correspond to the suggested uncertainty in the relationship of stable $(n_{\rm He,sep}, n_{\rm He^0,pump})$ points, with solid and dashed curves indicating the upper and lower bounds of $n_{\rm He,sep}$, respectively. These bounds correspond to $A = \{1.1 \times 10^{11}, 1.5 \times 10^{11}\}$, $\beta = 0.39$ (given that both $n_{\rm He,sep}$ and $n_{\rm He^0,pump}$ are in units of m⁻³). Assuming that the pumped helium flux $\Gamma_{\rm He}$ matches the reaction rate $\Gamma_{\rm min} = 5.33 \times 10^{20} \, {\rm s^{-1}}$ corresponding to $P_{\rm fus} = 1.5 \, {\rm GW}$ (the assumed lower bound for STEP fusion power performance [9]), eq. (2) can be used together with the suggested power law to yield the relationship $n_{\rm He,sep} = A(\Gamma_{\rm min}/S_{\rm He})^{\beta}$, as plotted in Fig. 5.d. Equating this with $n_{\rm He,sep} = (H_{98}^* - C_0 - C_\alpha \alpha_{\rm max})/C_n$, as derived in Section 3.2 (shown in Fig. 5.e for two different values of $\alpha_{\rm max}$) results in a lower limit of the helium pumping speed as a function of H_{98}^* and $\alpha_{\rm max}$ according to

$$S_{\text{He}} = \Gamma_{\text{min}} \left(\frac{AC_n}{H_{98}^* - C_0 - C_\alpha \alpha_{\text{max}}} \right)^{1/\beta}. \tag{3}$$

Fig. 5.f shows this relationship for $\alpha_{\rm max}=1.6$ and $\alpha_{\rm max}=2.5$ in purple and yellow, with the shaded areas being bound in H_{98}^* by the parameter space explored in the scan of Section 3.2 to avoid extrapolation of the linear fit. If the practical limit of the helium pumping speed is assumed to be around $50\,\mathrm{m}^3$ /s from a design point of view (dotted line in Fig. 5.f), the lower limit of H_{98}^* for sufficient pumped flux is between 1.336 and 1.356 for $\alpha_{\rm max}=1.6$, and between 1.299 and 1.319 for $\alpha_{\rm max}=2.5$. The flat-top scenario EC-HD [9] had an $H_{98}^*=1.349$, and an edge ballooning parameter $\alpha=1.498$. Inserting this into eq. (3) yields $S_{\rm He}=54.0\pm20.4\,\mathrm{m}^3$ /s, shown with the cyan error bar in Fig. 5.f. Consequently, it is possible that a viable operating point exists for the EC-HD scenario, but the operational space would be rather marginal, pushing the required pumping speed towards the upper technical limit.

Note that the derived value for the required EC-HD helium pumping speed $S_{\rm He}=54.0\pm20.4\,{\rm m}^3/{\rm s}$ corresponds to the pumping speed required for a pumped flux $\Gamma_{\rm He}=\Gamma_{\rm min}$, i.e., the same as the fusion reaction rate at $P_{\rm fus}=1.5\,{\rm GW}$. However, the actual fusion power for the EC-HD scenario is 1.68 GW. To derive the required pumping speed for this fusion rate, one cannot simply replace $\Gamma_{\rm min}$ with the corresponding increased flux, since

the coefficients C_0 , C_n and C_α include an implicit dependence of $P_{\rm fus}$, and the presented values have only been derived for $P_{\rm fus}=1.5\,{\rm GW}$.

4. CONCLUSIONS AND DISCUSSIONS

The presented studies have shown how important the pumping efficiency of helium ash is for fusion power performance of the STEP prototype power plant, using integrated core/SOL/divertor/pump modelling with JINTRAC. The lower limit of the helium pumping speed largely depends on the confinement and pedestal assumptions, which have been assessed quantitatively using the confinement factor and maximum edge ballooning parameter as proxies for these assumptions. The latest iteration of the flat-top scenario for the presented configuration predicts a minimum pumping speed of $54\,\mathrm{m}^3/\mathrm{s}$, with uncertainties $\sim\!20\,\mathrm{m}^3/\mathrm{s}$ in either direction. With increased understanding of the confinement and pedestal for STEP-relevant scenarios, the pumping requirements can be further specified. The predicted value is similar to what has been suggested for ITER helium pumping systems ($S_{\mathrm{He}} > 52\,\mathrm{m}^3/\mathrm{s}$ [5]). Note that ITER will be using carbon-coated cryopumps, which is of a different type than the turbomolecular pumps that have been planned for STEP.

The study was conducted in two steps. Using integrated core/SOL/divertor/pump modelling with JINTRAC, the helium pumping speed was varied to explore the correlation between helium pumping efficiency and core plasma operational space. A potential correlation between the average neutral density at the pump surfaces, $n_{\rm He^0,pump}$, and the helium density at the last closed flux surface, $n_{\rm He,sep}$, was identified, based on supposed stable points in $(n_{\rm He^0,pump},n_{\rm He,sep})$ -space that each pumping speed case oscillated around. The transport and confinement were not predicted in these simulations, but rather rescaled on feedback against a target $\beta_{\rm N}$ value, which provides stability and faster convergence of the scenarios. However, this effectively varies the heat confinement assumption between the cases, which is a key parameter in the fusion power performance for a given helium dilution. As a second step, a set of simulations using core-only JETTO modelling was conducted, in which the confinement and pedestal assumptions were varied independently. These simulations then yielded a relationship between helium separatrix density and confinement and pedestal assumptions at the lower bound of acceptable fusion power performance (1.5 GW). Combining the results from the two sets of simulations provides a complete picture of the pumping requirements as a function of confinement and pedestal assumptions.

While no definite conclusions could be drawn as to whether the presented pump and divertor design is viable for sufficient fusion power performance, the studies presents a framework within which confinement, pedestal, and helium pumping assumptions can be tested in combination for scenario and design viability. Since none of the JINTRAC simulations with varying helium pumping speed had reached full convergence, the correlation between $n_{\rm He^0,pump}$ and $n_{\rm He,sep}$ is rather uncertain. In addition, the suggested relationship $n_{\rm He,sep} \approx A n_{\rm He^0,pump}^{\beta}$ was solely based on observation of simulation results. A possible extension of the analysis would be to support a relationship between these parameters using a theoretical description of the SOL, e.g. a simplified 1D SOL model, or empirical scalings.

Regarding the derived relationship between confinement/pedestal assumptions and $n_{\rm He,sep}$, each of these assumptions were scanned by varying a single parameter. However, there are additional degrees of freedom in both confinement and pedestal assumptions that could be analysed in conjunction, such as the relative electron to ion heat confinement, relative heat to particle confinement, relative density to temperature pedestal heights, and relative electron to ion temperature pedestal heights. Each of these assumptions could be easily parametrised within the used models. The main challenge would be the computational demands to fully explore a 6-dimensional parameter space rather than a 2-dimensional one with sufficient range and resolution. However, 1D scans could be conducted separately for each assumption to give an indication of only the most important parameters for fusion power performance, which can then be selected in a more complete multi-dimensional scan to check for correlations between the model parameters.

ACKNOWLEDGEMENTS

This work has been funded by STEP, a major technology and infrastructure programme led by UK Industrial Fusion Solutions Ltd (UKIFS), which aims to deliver the UK's prototype fusion powerplant and a path to the commercial viability of fusion. To obtain further information on the data and models underlying this paper please contact PublicationsManager@ukaea.uk.

REFERENCES

[1] MEYER, H. (the STEP Plasma Team), Plasma burn-mind the gap, Phil. Trans. R. Soc. A **382** (2024) 20230406.

- [2] ROMANELLI, M., *et al.*, JINTRAC: A System of Codes for Integrated Simulation of Tokamak Scenarios, Plasma Fusion Res. **9** (2014) 340323.
- [3] HENDERSON, S.S., *et al.*, An overview of the STEP divertor design and the simple models driving the plasma exhaust scenario, Nucl. Fusion **65** (2025) 016033.
- [4] ZITO, A., *et al.*, Investigation of helium exhaust dynamics at the ASDEX Upgrade tokamak with full-tungsten wall, Nucl. Fusion **63** (2023) 096027.
- [5] PEARCE, R., *et al.*, ITER Vacuum Handbook, Appendices and Attachments, ITER Technical Report ITR-24-12 (2024).
- [6] CENACCHI, G. and TARONI, A., JETTO: A free boundary plasma transport code JET-IR(88)03 (1988). https://inis.iaea.org/collection/NCLCollectionStore/_Public/19/097/19097143.pdf.
- [7] SIMONINI, R., CORRIGAN, G., RADFORD, G., SPENCE, J., and TARONI, A., Models and Numerics in the Multi-Fluid 2-D Edge Plasma Code EDGE2D/U, Contrib. Plasma Phys. **34** (1994) 368.
- [8] REITER, D., BAELMANS, M., and BÖRNER, P., The EIRENE and B2-EIRENE Codes, Fusion Sci. Technol. 47 (2005) 172.
- [9] THOLERUS, E., *et al.*, Flat-top plasma operational space of the STEP power plant, Nucl. Fusion **64** (2024) 106030.
- [10] FICHTMÜLLER, M., CORRIGAN, G., RADFORD, G., SIMONINI, R., SPENCE, J. and TARONI, A., Multi-Species Developments in the EDGE2D Code, Contrib. Plasma Phys. **38** (1998) 284.
- [11] HOULBERG, W.A., SHAING, K.C., HIRSHMAN, S.P. and ZARNSTORFF, M.C., Bootstrap current and neoclassical transport in tokamaks of arbitrary collisionality and aspect ratio, Phys. Plasmas 4 (1997) 3230.
- [12] THOLERUS. E., *et al.*, Access and sustainment of ELMy H-mode operation for ITER pre-fusion power operation plasmas using JINTRAC, Nucl. Fusion **65** (2025) 036006.